New method to quantify hydrophobicity of non-enveloped virions in aqueous media by capillary zone electrophoresis

Guillaume Bastin, Christophe Gantzer, Guillaume Sautrey

Title:

New Method to Quantify Hydrophobicity of Non-enveloped Virions in Aqueous Media by Capillary Zone Electrophoresis

Authors:

Guillaume Bastin, Christophe Gantzer, Guillaume Sautrey*

Affiliation:

LCPME UMR 7564, Université de Lorraine – CNRS, 405 rue de Vandoeuvre 54600 Villers-lès-Nancy, France.

* **Corresponding author:**

Dr. Guillaume Sautrey,

Tel: +33 3 72 74 74 12.

E-mail address: guillaume.sautrey@univ-lorraine.fr

Keywords:

Bacteriophage; virion; hydrophobicity; non-enveloped virus; pH; capillary zone electrophoresis; SDS; aqueous media.

Abstract

The hydrophobicity of virions is a major physicochemical parameter regulating their dissemination in humans and the environment. But knowledge about potential factors modulating virion hydrophobicity is limited due to the lack of suitable quantifying methods. It has been recently shown that sodium dodecyl-sulfate (SDS) labels capsid hydrophobic domains in capillary zone electrophoresis of non-enveloped virions, altering their electrophoretic mobility (μ) in proportion to their hydrophobicity. This was exploited here to quantify the hydrophobicity of GA, Qβ and MS2 phages as a function of pH. By subtracting the native from the SDS-modified μ of phages, measured in the absence and presence of SDS, respectively, we defined a "hydrophobic index" increasing with virion hydrophobicity. Using this approach, we found that the virion hydrophobicity changes at a virion-specific pivotal pH. This procedure may be applied under various physicochemical conditions and to diverse non-enveloped virus families of significance to human health and the environment.

1. Introduction

The replication cycle of viruses includes an extracellular period during which viral particles, called virions, may reach the environment to reside for weeks/months. At this stage, the physicochemical surface properties of virions largely modulate their adhesion to diverse surfaces (Gerba, 1984). Notably, change in the electrical charge and/or hydrophobicity of virions in response to fluctuations in the environment (e.g. pH, temperature, or ionic strength) inevitably impact the fate of viruses. Therefore, understanding these physicochemical dynamics is important to predict transmission routes of viruses and to better control their dissemination as recently emphasized with the COVID-19 outbreak (Joonaki et al., 2020).

Both charge-charge and hydrophobic interactions cooperate by acting in a 'supralinear' way (Stefan and Le Novère, 2013) and therefore must be considered together when studying virion adhesion processes (Gerba, 1984). The overall electric charge of virions can be assessed by considering their isoelectric point (pHi) (Michen and Graule, 2010), i.e. the pH value at which the virion charge reverses. But the interpretation of pHi values may be unreliable in describing the ionization degree of virions beyond this equilibrium pH (Dika et al., 2015; Heffron and Mayer, 2021; Langlet et al., 2008a). The electrophoretic mobility (μ) of virions can provide quantitative information about their surface charge density outside their pHi (Heffron and Mayer, 2021). It is known that the electric charge of virions changes non-linearly as a function of pH (Armanious et al., 2016; Langlet et al., 2008a; Shi and Tarabara, 2018) and ionic strength (Dika et al., 2013b; Langlet et al., 2008a). The hydrophobicity of virions also varies between viruses (Armanious et al., 2016; Dika et al., 2013b; Shi and Tarabara, 2018), but the dynamics of virion hydrophobicity and potential physicochemical factors affecting it remain to be characterized. The pH of the virion environment may be such

a factor, as pH variations can induce structural rearrangements in the proteinaceous capsid (Roshal et al., 2019; Song et al., 2020), modifying the surface exposure of hydrophobic amino acid residues that should have an impact on virion hydrophobicity. The protonation/deprotonation equilibria of alkaline/acidic amino acid residues in the capsid are also expected to impact the hydrophobic/hydrophilic balance of virions (Dika et al., 2013b). Therefore, like electrical charge, the hydrophobicity of virions should be considered dynamically in response to pH variation.

The electrophoretic mobility μ of all electrically charged molecular species depends on their size-to-charge ratio. This is the separative principle of capillary zone electrophoresis (CZE) (Shintani, 1997). But for macromolecular assemblies like viruses, the charged surface leads to the formation of an electric double layer (EDL) and thus to a zeta potential (ζ) (Hunter, 1981a, 1981b). Therefore the molecular electrokinetic model of CZE becomes irrelevant with viruses (Kenndler, 2001). To describe the electromigration of virions in CZE, several electrokinetic theories can be applied depending on a ratio of the virion's radius R to the reciprocal of the Debye parameter K (i.e. the thickness of the EDL), the latter being influenced by the ionic strength I of the medium ($K \sim \sqrt{I}$). For moderate ionic strengths (i.e. 10-100 mM), the thickness of the EDL formed around a virion is much smaller than its radius. According to the Smoluchowsky electrokinetic model, the μ value of a virion becomes thus proportional to its ζ potential, itself being proportional to the virion's charge density and to the K value (Kenndler, 2001). Interestingly, it has been recently reported that adding an anionic amphiphilic compound, sodium dodecyl-sulfate (SDS), to the background electrolyte (BGE) used for CZE analyses resulted in a μ shift for MS2 and Qβ phages in comparison with similar SDS-free analyses (Sautrey et al., 2018). This effect has been shown to be related to non-polar interactions of the lipophilic tail of SDS

molecules with capsid hydrophobic domains, exposing in their stead the negatively charged hydrophilic head of SDS molecules, thereby increasing the negative charge density of virions. One can thus hypothesize that the more SDS changes the μ value of virions the more capsids have hydrophobic domains. Based on this line of thought, the SDS-induced shifting of μ values in CZE analyses of virions can be exploited to quantify virion hydrophobicity in aqueous media.

MS2, GA and Qβ are bacteriophages belonging to the *Leviviridae*. The virions consist of a positive single stranded RNA enclosed in an icosahedral capsid (27 nm diameter) made from 178 copies of a single coat protein (Golmohammadi et al., 1996, 1993; Tars et al., 1997). The capsids also include one copy of a maturation protein bound to the RNA genome and that is essential for the virions to be infectious (Cui et al., 2017; Dent et al., 2013). These bacteriophages infect *Escherichia coli* in the human or animal intestine; they are therefore sometimes released in feces and follow the fecal oral route to infect new hosts. Being structurally similar to most enteric viruses pathogenic to humans and following similar environmental routes, MS2, GA and Qβ are often used to predict the dissemination of waterborne enteric viruses in the environment and their accumulation in food products (Farkas et al., 2020; Hodgson et al., 2017). The persistence of phages *in vivo* is equally important in the context of their use in therapy situations (Serwer et al., 2021). The rate of their removal from blood by the reticuloendothelial system (Merril et al., 1996) involves the physicochemical adhesion of virions to the surface of cells specialized in blood clearing. For these purposes, MS2, GA and Qβ phages have been used as models for studying virion hydrophobicity (Armanious et al., 2016; Boudaud et al., 2012; Dika et al., 2013b; Langlet et al., 2008a). However, virion hydrophobicity was considered as a constant parameter, and its dynamics in response to environmental changes, notably pH

variations, remain to be evidenced in order to provide a comprehensive prediction of the dissemination of viruses in aqueous media.

The strategy here was thus to measure the SDS-induced shift in the μ value of MS2, GA and Qβ phages as a function of pH from 4 to 11 by CZE analyses performed in the absence and presence of 10 mM SDS. These shifts were determined by subtracting the native μ value ($\mu_{native}^{phage,\ pH}$) from the corresponding SDS-modified μ ($\mu_{SDS\text{-}modified}^{phage,\ pH}$) to quantify the hydrophobicity of virions by means of a 'hydrophobic index' (symbolized H_{pH}^{phage}). Importantly, all phosphate buffers used as BGE were prepared to ensure 10 mM ionic strength by adjusting the phosphate concentration according to the desired pH value, otherwise (i) changes in the Debye parameter K of the virions depending on the ionic strength of the medium are likely to interfere with the measurements (Kenndler, 2001; Langlet et al., 2008a), and (ii) phage aggregation often occurred beyond 100 mM ionic strength (Langlet et al., 2008a) may also interfere in measurements by preventing SDS binding to the virions buried within aggregates. Following this procedure, we found that the hydrophobicity of MS2, GA and Qβ phages changes suddenly at a phage-specific pivotal pH. This is possibly also true for other non-enveloped virus families and other physicochemical factors.

2. Materials and methods

2.1. Chemical and reagents

Phosphoric acid ≥ 85% (14.6 M), sodium dodecyl-sulfate (SDS), dimethyl sulfoxide (DMSO) and other reagents in analytical grade were from Sigma Aldrich (Saint Louis, USA). Ultrapure water was obtained in a Purelab Ultra MKII system from Elga (Le Plessis Robinson, France).

2.2. Production and purification of bacteriophages

MS2, GA and Qβ were all produced, purified and enumerated using described protocols (Bastin et al., 2020). The final concentrations of purified phage suspensions in 1 mM PBS (13.7 mM NaCl, 0.27 mM KCl, 1.0 mM Na_2HPO_4, 0.18 mM KH_2PO_4, pH 7.4) were 4×10^{13} PFU/mL for MS2, 1×10^{13} PFU/mL for Qβ, and 5×10^{12} PFU/mL for GA. The stock suspensions were stored at 4°C and away from light until use.

2.3. Capillary zone electrophoresis (CZE)

CZE experiments were performed on a PA 800 *Plus* Pharmaceutical Analysis System apparatus (SCIEX) equipped with a diode array UV/vis detector operating between 200 and 300 nm and located at the outlet side of the capillary. Data acquisition and processing were performed using the 32 Karat software supplied by SCIEX, and electropherograms at 214 nm were analyzed. A fused-silica capillary 75 µm internal diameter (Polymicro Technologies, Caudebec les Elboeuf, France), 30 cm total length (from the inlet to the outlet) and 20 cm effective length (from the inlet to the UV detection window) was employed. Capillary temperature was controlled by coolant at 25.0 °C. All solutions were filtered before use with a 0.45 µm pore size regenerated cellulose filter (Alltech, Templeuve, France). Analyses were accomplished using

156 phosphate buffers as background electrolytes (BGEs), supplemented or not with 10
157 mM SDS. The BGEs were prepared by diluting appropriate volume of 0.85% H_3PO_4
158 aqueous solution (146 mM) to reach the required concentration for a final 10 mM ionic
159 strength depending on the desired pH (please, read Appendix A for details), and
160 eventually by dissolving SDS powder in ultrapure water. The pH was adjusted with 1
161 M NaOH, and ultrapure water was added up to final volume.

162 A neutral marker was prepared by diluting pure DMSO (0.005% v/v) in ultrapure
163 water or in 10 mM SDS aqueous solution in order to measure the mobility μ_{EOF} of the
164 electroosmotic flow (EOF) for each analysis. The ionic strength of stock phage
165 suspensions was reduced by one-tenth dilution in ultrapure water or in 10 mM SDS
166 aqueous solution prior to analysis in order to avoid variable stacking effects within each
167 phage sample at the beginning of CZE runs. The final concentrations of viral samples
168 were 4×10^{12} PFU/mL for MS2, 1×10^{12} PFU/mL for Qβ and, 5×10^{11} PFU/mL for GA. For
169 CZE analyses of the three phages together (Fig. 1a and 2a), 5 µL of 10-fold diluted
170 phage suspensions were mixed directly into a vial prior to injection.

171 The analytical method consisted of successive rinses using 1 M NaOH (2 min),
172 ultrapure water (2 min) and BGE (2 min). Then, the DMSO and viral samples were
173 successively injected at the inlet side of the capillary in the hydrodynamic forward mode
174 under 0.5 psi pressure (3 s for DMSO solution then 5 s for viral suspension), both sides
175 of the capillary were immersed in BGE, and 10 kV voltage was applied (normal
176 polarity). The EOF is then oriented from the anodic inlet side to the detection window
177 near the cathodic outlet side. The virions, being negatively charged, are attracted to
178 the anode (i.e. by their electrophoretic mobility μ) while being pulled towards the
179 cathode by the EOF oriented in the opposite direction. Thus, virions migrate more
180 slowly than DMSO, and the more their negative charge density, the longer is their

migration time. All analyses were performed at least in triplicate in order to evaluate the residual standard deviation (RSD) for each measurement.

2.4. Mobility and hydrophobic index calculation

In CZE performed in normal polarity, each species injected at the inlet of the BGE-filled capillary are mobilized toward the detection window under the influence of a high voltage applied between both sides of the capillary. The migration velocity of the analytes is governed by their apparent mobility (μ_{app}) which can be determined from measurement of their migration time according to the following relation (Shintani, 1997):

$$\mu_{app} = \frac{L \times l}{\Delta V \times t_m} \quad (1)$$

where μ_{app} is the apparent mobility of the considered analyte, L is the capillary total length expressed in meter, l is the capillary effective length from the inlet to the detection window (meters), ΔV is the applied electrical potential expressed in volt and t_m is the migration time of the analyte expressed in seconds.

The apparent mobility of each analyte is so called because it is the outcome of two intrinsic mobilities, namely the electroosmotic mobility (μ_{eof}) and the electrophoretic mobility (μ) as shown in the following relation:

$$\mu_{app} = \mu + \mu_{eof} \quad (2)$$

where μ_{eof} is a driving force both for ionic and neutral species, which depends on the BGE composition, while μ is a specific feature of electrically charged analytes depicting their electrostatic attraction to either of the two electrodes located at the capillary extremities.

With neutral species like DMSO, where there are no cathodic or anodic attractions, μ is null. Such neutral species are therefore mobilized only according to the EOF, enabling determination of the μ_{eof} value from the relation (3) by combining the relations (1) and (2):

$$\mu_{app}^{DMSO} = \mu_{eof} = \frac{L \times l}{\Delta V \times t_m^{DMSO}} \quad (3)$$

where μ_{app}^{DMSO} is the apparent mobility of DMSO and t_m^{DMSO} is its migration time.

From a single run performed by co-injecting a DMSO sample as an EOF marker and a phage sample as an electrically charged entity, we applied relation (3) with the DMSO migration time to determine the μ_{eof} value while relation (1) was applied with the phage migration time to determine the μ_{app} of virions. Finally, according to relation (2), both relations (1) and (3) were combined to determine the μ of virions:

$$\mu^{virion} = \mu_{app}^{virion} - \mu_{app}^{DMSO} = \frac{L \times l}{\Delta V \times t_m^{virion}} - \frac{L \times l}{\Delta V \times t_m^{DMSO}} = \frac{L \times l}{\Delta V}\left(\frac{1}{t_m^{virion}} - \frac{1}{t_m^{DMSO}}\right) \quad (4)$$

where μ_{app}^{virion} and μ^{virion} are, respectively, the apparent and electrophoretic mobilities of a phage while t_m^{virion} is its migration time.

By applying relation (4), the native μ value of a phage at a given pH ($\mu_{native}^{phage,\ pH}$) was determined from CZE analysis without SDS, while the corresponding SDS-modified μ value ($\mu_{SDS\text{-}modified}^{phage,\ pH}$) was determined similarly from CZE analysis in the presence of 10 mM SDS. The hydrophobic index of phages as a function of pH (H_{pH}^{phage}) was calculated by subtracting the $\mu_{native}^{phage,\ pH}$ values from the $\mu_{SDS\text{-}modified}^{phage,\ pH}$ values, both expressed in terms of dimensionless quantities by normalizing mobilities with physical constants to undo their units (Radko et al., 2000):

$$H_{pH}^{phage} = \left(\mu_{SDS\text{-}modified}^{phage,\ pH} - \mu_{native}^{phage,\ pH}\right) \times \frac{3\eta e}{2\varepsilon kT} \quad (5)$$

where ε and η are respectively the permittivity and the viscosity of the BGE (taken as those of water that are 6.94×10^{-10} $F.m^{-1}$ and 8.90×10^{-4} Pa.s, respectively), k is the Boltzmann constant (1.38×10^{-23} $m^2.Kg.s^{-2}.K^{-1}$), T is the absolute temperature (298 K) and e is the electron charge (1.60×10^{-19} C).

2.5. Prediction of protein hydrophobicity from primary sequence analysis

Online protscale software from the expasy platform was used. The software can be found via the following internet link as it was on January 01, 2022: https://web.expasy.org/protscale/

For prediction of hydrophobicity, a seven amino acids smoothing average window was used for analysis by using the algorithm “Kyte and Doolittle”. Hydrophobic amino acid corresponding score can be found at the following internet link: https://web.expasy.org/protscale/pscale/Hphob.Doolittle.html

The sequences for capsid protein of GA, Qβ and MS2 phages were all from the UniProtKB data base with the following reference numbers: GA: P07234 (CAPSD_BPGA); MS2: P03612 (CAPSD_BPMS2); Qβ: P03615 (CAPSD_BPQBE).

3. Results and discussion

3.1. CZE assays with SDS-free BGEs: native electrophoretic mobilities

To illustrate the accuracy achieved by electrophoretic mobility measurement in CZE, a sample containing the three phages MS2, Qβ and GA was analyzed at pH 7 by co-injection with an aqueous solution of DMSO (used as the EOF marker). Each phage was detected as a single narrow peak, indicating no alteration of virions by the process of electrophoresis (Sautrey et al., 2018), and at a repeatable migration time of 1.75, 2.26 and 3.42 min for GA, Qβ and MS2, respectively (Fig. 1a). Peaks identification was made by individually analyzing each phage, which resulted in the same migration times as when pooled. All three phages were slower than DMSO at pH 7 (Fig. 1a), indicating a negative $\mu_{native}^{phage,\ 7}$ that is opposed to the EOF and signifies that virions are negatively charged (see Section 2.3). This is consistent with a previous study (Michen and Graule, 2010). Focusing on individual phages, GA was faster than Qβ, which is much faster than MS2 (Fig. 1a). This indicates $\mu_{native}^{MS2,\ 7} << \mu_{native}^{Q\beta,\ 7} < \mu_{native}^{GA,\ 7}$ (see Section 2.4 for details of data processing), suggesting the negative charge density order MS2>>Qβ>GA. This order is inconsistent with previous reports in which the negative charge density of MS2, Qβ and GA were similar at pH 7 (Dika et al., 2013b; Langlet et al., 2008a; Shirasaki et al., 2009). The difference may be due to disparities in the protocols in preparing the viral samples prior to electrophoretic mobility measurements (e.g. purification methods may impact the virion surface properties) (Dika et al., 2013a; Langlet et al., 2008a; Shi and Tarabara, 2018).

Each phage was then individually analyzed by co-injection with DMSO and using SDS-free BGEs at a pH range from 4 to 11 (all at 10 mM ionic strength). Importantly, the electric current intensities measured in the capillary during CZE analysis were similar (Fig. S1) indicating equivalent ionic strengths for all BGEs (Kuhn and

Hoffstetter-Kuhn, 1993). From these experiments, the native electrophoretic mobility $\mu_{native}^{phage,\ pH}$ of MS2, Qβ and GA phages was plotted against pH (Fig. 1b). However, on both sides of the pH range examined, the electrophoretic mobility measurement became unreliable for all three phages (residual standard deviation ~ 25%, n=3) due to poorly repeatable migration times. At pH 4, near the isoelectric point of these phages (Michen and Graule, 2010), the electrophoretic mobility of virions and the EOF mobility should tend to zero. This results in a very slow migration of both virions and DMSO (Fig. S2), which is detrimental to their separation and impairs the measurement of migration times required to calculate the electrophoretic mobility of virions.

The low precision in measurements at pH 11 is more difficult to explain and should be the subject of further study. It can be hypothesized that increasing pH values reduces the positive charges of protein domains near the RNA-coat protein interface, thus destabilizing viral particle assembly. Moreover, the more alkaline the media the more RNA spontaneously hydrolyses (Bock, 1967). This pH sensitivity has even been exploited to 'empty' MS2 virions of their RNA (Hooker et al., 2004). Since the electrokinetic properties of phages can, in some cases, be affected by the internal RNA of virions (Dika et al., 2011; Langlet et al., 2008b), RNA spontaneous hydrolysis at high pH may be responsible for the lack of precision at pH 11.

An optimal pH range was thus delimited from 5 to 10 at which the peaks of phages and DMSO were well resolved with repeatable migration times, allowing an accurate determination of $\mu_{native}^{phage,\ pH}$ (RSD lower than 5%, n=3). MS2, GA and Qβ are characterized by negative $\mu_{native}^{phage,\ pH}$ values that decreases with rising pH, clearly showing the dynamic of the charge density of virions as a function of pH (Fig. 1b). MS2 virions are more anionic than GA and Qβ virions at all pH levels examined as indicated

by the low $\mu_{native}^{MS2,\ pH}$ values (Fig. 1b, red) in comparison with $\mu_{native}^{GA,\ pH}$ and $\mu_{native}^{Q\beta,\ pH}$ values (Fig. 1b, green and blue, respectively).

3.2. CZE assays with SDS-containing BGEs: SDS-modified electrophoretic mobilities

When performing CZE analyses in the presence of 10 mM SDS, the migration order of MS2, Qβ and GA phages was reversed, as compared to SDS-free conditions. Indeed, while Qβ and GA migrated faster than MS2 without SDS at pH 7 (Fig. 1a), they are slower than MS2 in SDS-containing BGE (Fig. 2a). Quantitatively, the electrophoretic mobility of MS2 virions only decreased from -3.09×10^{-8} $m^2.V^{-1}.s^{-1}$ without SDS to -3.23×10^{-8} $m^2.V^{-1}.s^{-1}$ with SDS (20% decrease) indicating low interactions between SDS molecules and MS2 virions. In contrast, the electrophoretic mobility of Qβ and GA virions decreased significantly, from -1.35×10^{-8} $m^2.V^{-1}.s^{-1}$ to -3.66×10^{-8} $m^2.V^{-1}.s^{-1}$ for Qβ (177% decrease) and from -0.48×10^{-8} $m^2.V^{-1}.s^{-1}$ to -3.79×10^{-8} $m^2.V^{-1}.s^{-1}$ for GA (301% decrease). This indicates that SDS strongly interact with GA and much less with Qβ virions. Furthermore, since the larger the SDS-induced electrophoretic mobility decrease, the more hydrophobic the virions (Sautrey et al., 2018), these results suggest the hydrophobicity sequence GA>Qβ>MS2 consistently with earlier reports (Armanious et al., 2016; Dika et al., 2013b).

The SDS-modified electrophoretic mobility ($\mu_{SDS\text{-}modified}^{phage,\ pH}$) of MS2, Qβ and GA was plotted against pH (Fig. 2b). Note that $\mu_{SDS\text{-}modified}^{GA,\ pH}$ and $\mu_{SDS\text{-}modified}^{Q\beta,\ pH}$ values are lower than $\mu_{SDS\text{-}modified}^{MS2,\ pH}$ regardless of pH, except for Qβ at pH 5, indicating higher negative surface charge densities for GA and Qβ than for MS2 virion in the presence of SDS. The $\mu_{SDS\text{-}modified}^{phage,\ pH}$ values variation against pH is irregular for each phage and interesting

features can be observed. First, the $\mu_{SDS\text{-}modified}^{MS2,\ pH}$ and $\mu_{SDS\text{-}modified}^{GA,\ pH}$ values decrease almost linearly and similarly from pH 5 to 7 (Fig. 2b, red and green, respectively), while the $\mu_{SDS\text{-}modified}^{Q\beta,\ pH}$ value also decreases from pH 5 to 8 but more sharply (Fig. 2b, blue). Second, the $\mu_{SDS\text{-}modified}^{MS2,\ pH}$ value remains fairly stable from pH 7 to 10 (Fig. 2b, red), while the $\mu_{SDS\text{-}modified}^{GA,\ pH}$ and $\mu_{SDS\text{-}modified}^{Q\beta,\ pH}$ values suddenly increase at pH 8 and 9 respectively, and then decrease again until pH 10 (Fig. 2b, green and blue, respectively). Overall, these data highlight that virion hydrophobicity varies non-linearly with pH, but this dynamic is different for each phage.

3.3. SDS-free versus SDS-containing analyses: Phage hydrophobic index

The $\mu_{SDS\text{-}modified}^{phage,\ pH}$ values alone are not sufficient to assess the hydrophobicity of virions because their surface charge density in the presence of SDS is obviously related to both the ionizable residues of the proteinaceous capsid and to the SDS molecules bound to the capsid. The native ionization of virions must thus be extracted from their SDS-modified charge density to quantify their hydrophobicity. The 'hydrophobic index' of phages depending on pH (H_{pH}^{phage}) can be calculated by subtracting the $\mu_{native}^{phage,\ pH}$ values from the associated $\mu_{SDS\text{-}modified}^{phage,\ pH}$ values, and used to describe the hydrophobicity of phages. Both mobilities should be expressed in terms of reduced mobilities (Radko et al., 2000), to result in dimensionless H_{pH}^{phage} values that can be easily compared between any non-enveloped virions (see Section 2.4). Following this definition, H_{pH}^{phage} values start from 0 and increase with hydrophobicity. As shown in Fig. 3a, H_7^{MS2} is 0.10±0.11 suggesting a very low hydrophobicity of MS2 virions at pH 7. In contrast, $H_7^{Q\beta}$ and H_7^{GA} are 1.73±0.14 and 2.48±0.13, respectively.

These results modify the previously suggested hydrophobic sequence (Armanious et al., 2016; Dika et al., 2013b) to GA>Qβ>>MS2.

The very low value of H_7^{MS2} is intriguing in comparison to the higher H_7^{GA} value. Indeed, the MS2 and GA phages are very close in the evolutionary tree (Bollback and Huelsenbeck, 2001) and in their structures (Pumpens et al., 2016). Based on this reasoning, the theoretical hydrophobicity of the two capsid proteins of MS2 and GA phages was determined from their primary sequences (Fig. 4). Notably, the first 60 amino acids (of ~130 for both phages) are rather hydrophilic, while the C-terminal 70 amino acids are rather hydrophobic. Interestingly, the hydrophobic residues are present in longer stretches in the GA capsid protein (Fig. 4, solid line) than in MS2 (Fig. 4, dotted line). We thus suggest that the hydrophobic domains on the surface of MS2 virions may be too small to allow the binding of the relatively bulky SDS molecules, especially if they form micellar aggregates or other supramolecular assemblies (Sautrey et al., 2018). Future investigations could focus on testing other amphiphilic probes to increase the sensitivity of this method. Nevertheless, the theoretical hydrophobicity of a virion deduced from the primary sequence of its capsid protein is not correlated with that experimentally observed (Heldt et al., 2017), possibly because the internal RNA and the RNA-capsid protein interface may affect the physicochemical surface properties of virions (Dika et al., 2011; Langlet et al., 2008b).

The hydrophobic index of phages (H_{pH}^{phage}) was also determined from pH 5 to 10 (Fig. 3b). Interestingly, the H_{pH}^{phage} values are fairly stable for all three phages but only outside of a narrow pivotal pH range where values change suddenly. As shown in Fig. 3b (green), H_{pH}^{GA} decreases slightly from pH 5 to 7 (5% per pH unit) and from pH 8 to 10 (8% per pH unit), while a sharp decrease occurs between pH 7 and 8 (26% decrease). Similarly, $H_{pH}^{Q\beta}$ (Fig. 3b, blue) is almost unchanged from pH 5 to 8 and from

9 to 10 (<3% per pH unit), whereas a sharp drop occurs between pH 8 and 9 (31% decrease). Lastly, H_{pH}^{MS2} (Fig. 3b, red) drops from pH 5 to 6 (68%) but is then stable from pH 6 to 10. These data indicate a pivotal pH at which the hydrophobicity of virions decreases sharply and which is specific for each phage. This has not been observed using other methodologies or other non-enveloped viruses, and may be indicative of a structural rearrangement of virions in response to pH changes that affects hydrophobic domains on the capsid (Roshal et al., 2019; Song et al., 2020). Note that the pivotal pH values of hydrophobicity do not match the isoelectric point of these phages, which is below pH 4 (Michen and Graule, 2010), and that the curves of H_{pH}^{GA} and $H_{pH}^{Q\beta}$ versus pH do not overlap with the corresponding curves of native electrophoretic mobility (Fig. 5, middle and right panels). This supports the idea that the hydrophobicity dynamics of virions is not solely related to the ionization of the capsid, especially since other constituents, notably internal RNA, play a role in their structuring (Koning et al., 2016). Conversely, the H_{pH}^{MS2} versus pH curve overlaps the corresponding curve of native electrophoretic mobility (Fig. 5, left panel). This could be due to the low hydrophobicity of MS2 virions, at any pH, in comparison with Qβ and GA (Fig. 3a and 3b). Our observation of a pivotal pH of virion hydrophobicity requires further study to explain the phenomenon at a molecular level.

The finding of the pivotal pH of hydrophobicity means that minor pH variations may have a strong impact on the adhesion of virions onto surfaces, and therefore on their dissemination in both the environment and living organisms. For example, enteric virions have been shown to accumulate on riverbed sediments where they can be "stored" and released later to infect a new host (Bosch et al., 2006; Rao et al., 1986). These adsorption/desorption processes depend on both the electrical charge and hydrophobicity of virions (Fauvel et al., 2019), both varying with pH as we have shown

here for hydrophobicity. Moreover, the change in hydrophobicity of GA and MS2 at different pH values may help explain discrepancies in their behavior at interfaces when comparing the removal efficiency of virions from aqueous media ranging from pH 7.6 to 8.2 (Boudaud et al., 2012) versus their adhesion on hydrophobic surfaces under controlled pH conditions (Dika et al., 2013b). This clearly shows that further understanding how virion hydrophobicity varies, including pH but also other factors e.g., temperature (Brié et al., 2016), is essential to improve the process of water decontamination. Enteric virus pollution in water remains a major cause of viral outbreaks responsible for millions of infections in humans every year (Upfold et al., 2021). Note that the pH variation in virion hydrophobicity also may impact non-specific interactions with all kinds of biological components *in vivo*, especially if the virions pivotal pH of hydrophobicity is in a physiological pH range. For example, the entrapment of in-blood phages by the reticuloendothelial system may need to be controlled to ensure success during phage therapy (Merril et al., 1996). The persistence of virions in blood is indeed variable even for closely related phages (Serwer et al., 2021), just as we observed a marked difference in the hydrophobicity features of MS2 and GA phages. The measurement of virion hydrophobicity and the determination of a pivotal pH should thus be integrated into the framework of future studies dealing with the survival of phages in blood, their infectivity and their pathogenicity, and more generally with their dissemination in the human body.

4. Conclusion

The hydrophobicity of three non-enveloped virions was quantified here as a function of pH by using SDS to label capsid hydrophobic domains and CZE as sensing technique. This relatively simple and fast procedure can be applied under various physicochemical conditions in order to identify factors affecting virion hydrophobicity. The hydrophobic index defined here could be adopted as a standard parameter in describing the hydrophobicity of non-enveloped viruses. The virion hydrophobicity changes at a virion-specific pivotal pH require further investigation as its existence may reflect unknown structural dynamics of virions and could have broad implications in their pathogenicity and dissemination. This report concerns only non-enveloped +ssRNA icosahedral viruses but the approach developed can also be applied to other and diverse virus families of significance to human health and the environment.

Appendix A

The BGEs used in this study were prepared to keep a constant ionic strength (10 mM) regardless of pH. The total phosphate concentration as well as the corresponding volume of 0.85% H_3PO_4 aqueous stock solution (146 mM) required for 200 mL of BGE are reported in Table A1 as a function of pH. Briefly, the required volume of 0.85% H_3PO_4 was taken, 150 mL pure water was added and the pH was adjusted with 1 M NaOH; the final volume was adjusted with pure water.

Table A1. Total phosphate concentration and corresponding volume of 0.85% H_3PO_4 aqueous solution (146 mM) required for the preparation of 200 mL of 10 mM ionic strength BGEs.

pH	Total phosphate concentration (mM)	Volume of H_3PO_4 0,85% (mL)
4	10.13	13.86
5	9.88	13.52
6	9.62	13.16
7	8.94	12.23
8	7.50	10.26
9	5.64	7.72
10	4.29	5.87
11	3.67	5.02

Acknowledgement

We gratefully acknowledge Pr R. Duval, faculty director of Faculté de Pharmacie de Nancy (Université de Lorraine, Nancy, France), for access to the capillary electrophoresis instrument and Pr. I. Clarot (EA 3452 CITHEFOR, Université de Lorraine, Nancy, France) for valuable discussions. We thank also J. Challant (UMR 7564 LCPME, CNRS-Université de Lorraine, Nancy, France) for assistance in phages production and purification as well as the colleagues of the laboratory for the English revision of the manuscript. Finally, we acknowledge the anonymous Reviewers as well as Ian J. Molineux (Editor) for their much-appreciated contributions in improving this paper.

CRediT authors contribution statement

Guillaume Bastin: Conceptualization, Resources, Formal analysis, Writing – Original Draft, Visualization. **Christophe Gantzer:** Conceptualization, Writing – Review & Editing. **Guillaume Sautrey:** Conceptualization, Methodology, Validation, Formal analysis, Investigation, Resources, Writing – Original Draft, Writing – Review & Editing, Visualization, Supervision, Project administration.

Declaration of competing interest

The authors have no conflicts of interest.

Funding

This work was supported by French Ministry of Higher Education and Research and the French National Scientific Research Center (CNRS), as well as the University of Lorraine. This research received no external funding.

References

Armanious, A., Aeppli, M., Jacak, R., Refardt, D., Sigstam, T., Kohn, T., Sander, M., 2016. Viruses at Solid-Water Interfaces: A Systematic Assessment of Interactions Driving Adsorption. Environ. Sci. Technol. 50, 732–743. https://doi.org/10.1021/acs.est.5b04644

Bastin, G., Loison, P., Vernex-Loset, L., Dupire, F., Challant, J., Majou, D., Boudaud, N., Krier, G., Gantzer, C., 2020. Structural Organizations of Qβ and MS2 Phages Affect Capsid Protein Modifications by Oxidants Hypochlorous Acid and Peroxynitrite. Front. Microbiol. 11, 1–13. https://doi.org/10.3389/fmicb.2020.01157

Bock, R.M., 1967. [29] Alkaline hydrolysis of RNA. Methods Enzymol. 12, 224–228. https://doi.org/10.1016/s0076-6879(67)12035-1

Bollback, J.P., Huelsenbeck, J.P., 2001. Phylogeny, genome evolution, and host specificity of single-stranded RNA bacteriophage (family Leviviridae). J. Mol. Evol. 52, 117–128. https://doi.org/10.1007/s002390010140

Bosch, A., Pintó, R.M., Abad, F.X., 2006. Survival and Transport of Enteric Viruses in the Environment, in: Goyal, S.M. (Ed.), Viruses in Foods. Springer US, Boston, MA, pp. 151–187. https://doi.org/10.1007/0-387-29251-9_6

Boudaud, N., Machinal, C., David, F., Fréval-Le Bourdonnec, A., Jossent, J., Bakanga, F., Arnal, C., Jaffrezic, M.P., Oberti, S., Gantzer, C., 2012. Removal of MS2, Qβ and GA bacteriophages during drinking water treatment at pilot scale. Water Res. 46, 2651–2664. https://doi.org/10.1016/j.watres.2012.02.020

Brié, A., Bertrand, I., Meo, M., Boudaud, N., Gantzer, C., 2016. The Effect of Heat on the Physicochemical Properties of Bacteriophage MS2. Food Environ. Virol. 8, 251–261. https://doi.org/10.1007/s12560-016-9248-2

Cui, Z., Gorzelnik, K. V., Chang, J.Y., Langlais, C., Jakana, J., Young, R., Zhang, J., 2017. Structures of Qβ virions, virus-like particles, and the Qβ–MurA complex reveal internal coat proteins and the mechanism of host lysis. Proc. Natl. Acad. Sci. U. S. A. 114, 11697–11702. https://doi.org/10.1073/pnas.1707102114

Dent, K.C., Thompson, R., Barker, A.M., Hiscox, J.A., Barr, J.N., Stockley, P.G., Ranson, N.A., 2013. The asymmetric structure of an icosahedral virus bound to its receptor suggests a mechanism for genome release. Structure 21, 1225–1234. https://doi.org/10.1016/j.str.2013.05.012

Dika, C., Duval, J.F.L., Francius, G., Perrin, A., Gantzer, C., 2015. Isoelectric point is an inadequate descriptor of MS2, Phi X 174 and PRD1 phages adhesion on abiotic surfaces. J. Colloid Interface Sci. 446, 327–334. https://doi.org/10.1016/j.jcis.2014.08.055

Dika, C., Duval, J.F.L., Ly-Chatain, H.M., Merlin, C., Gantzer, C., 2011. Impact of internal RNA on aggregation and electrokinetics of viruses: comparison between MS2 phage and corresponding virus-like particles. Appl. Environ. Microbiol. 77, 4939–48. https://doi.org/10.1128/AEM.00407-11

Dika, C., Gantzer, C., Perrin, A., Duval, J.F.L., 2013a. Impact of the virus purification protocol on aggregation and electrokinetics of MS2 phages and corresponding virus-like particles. Phys. Chem. Chem. Phys. 15, 5691–5700. https://doi.org/10.1039/c3cp44128h

Dika, C., Ly-Chatain, M.H., Francius, G., Duval, J.F.L., Gantzer, C., 2013b. Non-DLVO adhesion of F-specific RNA bacteriophages to abiotic surfaces: Importance of surface roughness, hydrophobic and electrostatic interactions. Colloids Surfaces A Physicochem. Eng. Asp. 435, 178–187. https://doi.org/10.1016/j.colsurfa.2013.02.045

Farkas, K., Walker, D.I., Adriaenssens, E.M., McDonald, J.E., Hillary, L.S., Malham, S.K., Jones, D.L., 2020. Viral indicators for tracking domestic wastewater contamination in the aquatic environment. Water Res. 181, 115926. https://doi.org/10.1016/j.watres.2020.115926

Fauvel, B., Cauchie, H.M., Gantzer, C., Ogorzaly, L., 2019. Influence of physico-chemical characteristics of sediment on the in situ spatial distribution of F-specific RNA phages in the riverbed. FEMS Microbiol. Ecol. 95, 1–11. https://doi.org/10.1093/femsec/fiy240

Gerba, C.P., 1984. Applied and Theoretical Aspects of Virus Adsorption to Surfaces. Adv. Appl. Microbiol. 30, 133–168. https://doi.org/10.1016/S0065-2164(08)70054-6

Golmohammadi, R., Fridborg, K., Bundule, M., Valegård, K., Liljas, L., 1996. The crystal structure of bacteriophage Qβ at 3.5 å resolution. Structure 4, 543–554. https://doi.org/10.1016/S0969-2126(96)00060-3

Golmohammadi, R., Valegård, K., Fridborg, K., Liljas, L., 1993. The Refined Structure of Bacteriophage MS2 at 2·8 Å Resolution. J. Mol. Biol. https://doi.org/10.1006/jmbi.1993.1616

Heffron, J., Mayer, B.K., 2021. Virus Isoelectric Point Estimation: Theories and Methods. Appl. Environ. Microbiol. 87, 1–17. https://doi.org/10.1128/AEM.02319-20

Heldt, C.L., Zahid, A., Vijayaragavan, K.S., Mi, X., 2017. Experimental and computational surface hydrophobicity analysis of a non-enveloped virus and proteins. Colloids Surfaces B Biointerfaces 153, 77–84. https://doi.org/10.1016/j.colsurfb.2017.02.011

Hodgson, K.R., Torok, V.A., Turnbull, A.R., 2017. Bacteriophages as enteric viral indicators in bivalve mollusc management. Food Microbiol. 65, 284–293. https://doi.org/10.1016/j.fm.2017.03.003

Hooker, J.M., Kovacs, E.W., Francis, M.B., 2004. Interior Surface Modification of Bacteriophage MS2. J. Am. Chem. Soc. 126, 3718–3719. https://doi.org/10.1021/ja031790q

Hunter, R.J., 1981a. Chapter 2 - Charge and Potential Distribution at Interfaces, in: HUNTER, R.J. (Ed.), Zeta Potential in Colloid Science. Academic Press, pp. 11–58. https://doi.org/https://doi.org/10.1016/B978-0-12-361961-7.50006-7

542 Hunter, R.J., 1981b. Chapter 3 - The Calculation of Zeta Potential, in: HUNTER, R.J.
543 (Ed.), Zeta Potential in Colloid Science. Academic Press, pp. 59–124.
544 https://doi.org/https://doi.org/10.1016/B978-0-12-361961-7.50007-9

545 Joonaki, E., Hassanpouryouzband, A., Heldt, C.L., Areo, O., 2020. Surface
546 Chemistry Can Unlock Drivers of Surface Stability of SARS-CoV-2 in a Variety of
547 Environmental Conditions. Chem 6, 2135–2146.
548 https://doi.org/10.1016/j.chempr.2020.08.001

549 Kenndler, E., 2001. Capillary electrophoresis of macromolecular biological
550 assemblies : bacteria and viruses 20, 543–551.

551 Koning, R.I., Gomez-Blanco, J., Akopjana, I., Vargas, J., Kazaks, A., Tars, K.,
552 Carazo, J.M., Koster, A.J., 2016. Asymmetric cryo-EM reconstruction of phage
553 MS2 reveals genome structure in situ. Nat. Commun. 7, 1–6.
554 https://doi.org/10.1038/ncomms12524

555 Kuhn, R., Hoffstetter-Kuhn, S., 1993. Capillary Electrophoresis: Principles and
556 Practice. Springer-Verlag, Berlin. https://doi.org/10.1007/978-3-642-78058-5

557 Langlet, J., Gaboriaud, F., Duval, J.F.L., Gantzer, C., 2008a. Aggregation and
558 surface properties of F-specific RNA phages: Implication for membrane filtration
559 processes. Water Res. 42, 2769–2777.
560 https://doi.org/10.1016/j.watres.2008.02.007

561 Langlet, J., Gaboriaud, F., Gantzer, C., Duval, J.F.L., 2008b. Impact of chemical and
562 structural anisotropy on the electrophoretic mobility of spherical soft multilayer
563 particles: the case of bacteriophage MS2. Biophys. J. 94, 3293–3312.
564 https://doi.org/10.1529/biophysj.107.115477

565 Merril, C.R., Biswas, B., Carlton, R., Jensen, N.C., Creed, G.J., Zullo, S., Adhya, S.,
566 1996. Long-circulating bacteriophage as antibacterial agents. Proc. Natl. Acad.
567 Sci. U. S. A. 93, 3188–3192. https://doi.org/10.1073/pnas.93.8.3188

568 Michen, B., Graule, T., 2010. Isoelectric points of viruses. J. Appl. Microbiol. 109,
569 388–397. https://doi.org/10.1111/j.1365-2672.2010.04663.x

570 Pumpens, P., Renhofa, R., Dishlers, A., Kozlovska, T., Ose, V., Pushko, P., Tars, K.,
571 Grens, E., Bachmann, M.F., 2016. The true story and advantages of RNA phage
572 capsids as nanotools. Intervirology 59, 74–100.
573 https://doi.org/10.1159/000449503

574 Radko, S.P., Stastna, M., Chrambach, A., 2000. Size-Dependent Electrophoretic
575 Migration and Separation of Liposomes by Capillary Zone Electrophoresis in
576 Electrolyte Solutions of Various Ionic Strengths 72, 5955–5960.

577 Rao, V.C., Metcalf, T.G., Melnick, J.L., 1986. Human viruses in sediments, sludges,
578 and soils. Bull. World Health Organ. 64, 1–14.
579 https://doi.org/10.1201/9780429270475

580 Roshal, D., Konevtsova, O., Božič, A.L., Podgornik, R., Rochal, S., 2019. pH-induced
581 morphological changes of proteinaceous viral shells 1–9.
582 https://doi.org/10.1038/s41598-019-41799-6

583 Sautrey, G., Brié, A., Gantzer, C., Walcarius, A., 2018. MS2 and Qβ bacteriophages
584 reveal the contribution of surface hydrophobicity on the mobility of non-
585 enveloped icosahedral viruses in SDS-based capillary zone electrophoresis.
586 Electrophoresis 39, 377–385. https://doi.org/10.1002/elps.201700352

587 Serwer, P., Wright, E.T., De La Chapa, J., Gonzales, C.B., 2021. Basics for improved
588 use of phages for therapy. Antibiotics 10, 1–12.
589 https://doi.org/10.3390/antibiotics10060723

590 Shi, H., Tarabara, V. V., 2018. Charge, size distribution and hydrophobicity of
591 viruses: Effect of propagation and purification methods. J. Virol. Methods 256,
592 123–132. https://doi.org/10.1016/j.jviromet.2018.02.008

593 Shintani, H., 1997. Handbook of Capillary Electrophoresis Applications. Springer,
594 Dordrecht. https://doi.org/https://doi.org/10.1007/978-94-009-1561-9

595 Shirasaki, N., Matsushita, T., Matsui, Y., Urasaki, T., Ohno, K., 2009. Comparison of
596 behaviors of two surrogates for pathogenic waterborne viruses, bacteriophages
597 Q?? and MS2, during the aluminum coagulation process. Water Res. 43, 605–
598 612. https://doi.org/10.1016/j.watres.2008.11.002

599 Song, C., Takai-Todaka, R., Miki, M., Haga, K., Fujimoto, A., Ishiyama, R., Oikawa,
600 K., Yokoyama, M., Miyazaki, N., Iwasaki, K., Murakami, K., Katayama, K.,
601 Murata, K., 2020. Dynamic rotation of the protruding domain enhances the
602 infectivity of norovirus. PLoS Pathog. 16, 1–24.
603 https://doi.org/10.1371/journal.ppat.1008619

604 Stefan, M.I., Le Novère, N., 2013. Cooperative Binding. PLoS Comput. Biol. 9, 2–7.
605 https://doi.org/10.1371/journal.pcbi.1003106

606 Tars, K., Bundule, M., Fridborg, K., Liljas, L., 1997. The crystal structure of
607 bacteriophage GA and a comparison of bacteriophages belonging to the major
608 groups of Escherichia coli leviviruses. J. Mol. Biol. 271, 759–773.

609 Upfold, N.S., Luke, G.A., Knox, C., 2021. Occurrence of Human Enteric Viruses in
610 Water Sources and Shellfish: A Focus on Africa, Food and Environmental
611 Virology. Springer US. https://doi.org/10.1007/s12560-020-09456-8

612

613

Fig. 1. Electrokinetic properties of phages in SDS-free CZE. (**a**) Representative electropherogram obtained at pH 7 with a pooled sample of MS2 (■), Qβ (●) and GA (▲) co-injected with a 0.005% v/v DMSO aqueous solution (✱). The inset is an enlargement near the peaks of DMSO (✱) and GA (▲). BGE: 8.94 mM phosphoric acid adjusted to pH 7.0 (10 mM ionic strength). (**b**) pH-dependent variations in the native electrophoretic mobility $\mu_{native}^{phage,\ pH}$ of MS2 (■), Qβ (●) and GA (▲) measured by means of CZE analyses performed with different BGEs ranging from pH 4 to 11 (all 10 mM ionic strength). The dotted line indicates the isoelectric point ($\mu_{native}^{phage,\ pH}$ = 0). Error bars are standard deviation (n=3).

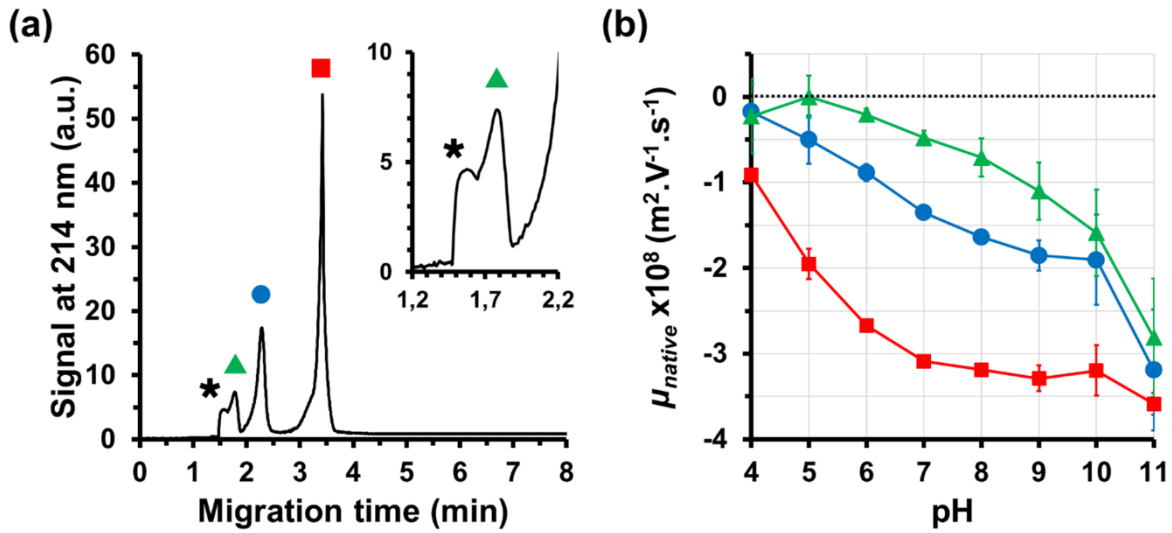

Fig. 2. Electrokinetic properties of phages in SDS-containing CZE. (**a**) Representative electropherogram obtained at pH 7 with a pooled sample of MS2 (■), Qβ (●) and GA (▲) co-injected with a 0.005% v/v DMSO aqueous solution (✱). BGE: 8.94 mM phosphoric acid adjusted to pH 7.0 (10 mM ionic strength) supplemented with 10 mM SDS. (**b**) pH-dependent variations in the SDS-modified electrophoretic mobility $\mu_{SDS\text{-}modified}^{phage,\ pH}$ of MS2 (■), Qβ (●) and GA (▲) obtained as for Figure 1, but in the presence of 10 mM SDS. Error bars are standard deviation (n=3).

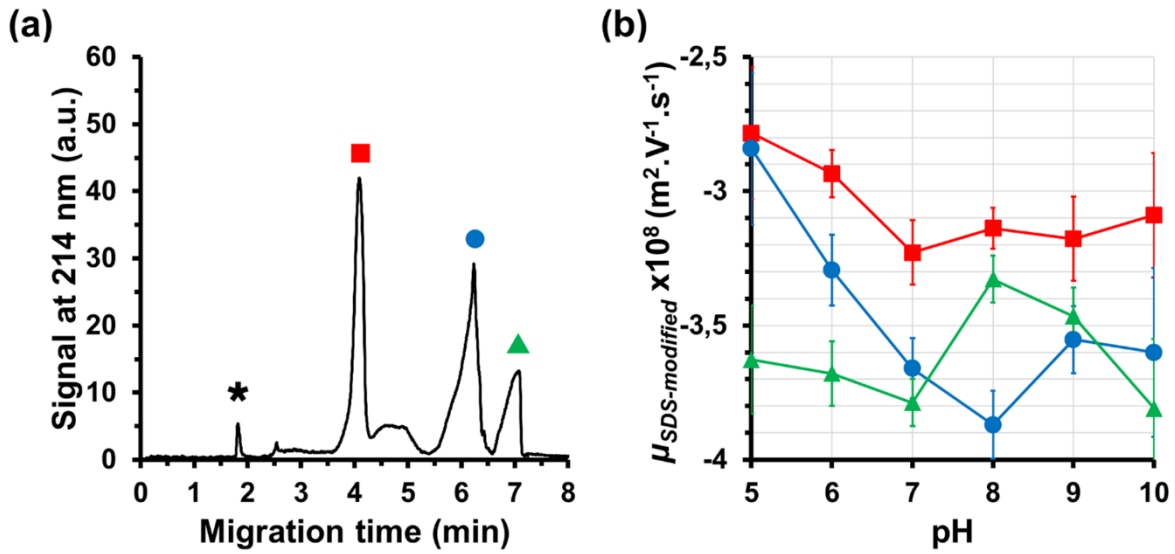

Fig. 3. Assessment of phages hydrophobicity as a function of pH. (**a**) comparison of the hydrophobic indexes found at pH 7 for MS2 (red), Qβ (blue) and GA (green). (**b**) pH-dependent variations in the hydrophobic index of MS2 (■), Qβ (●) and GA (▲). Error bars are the sum of standard deviations related to the electrophoretic mobilities of native and SDS-modified phages.

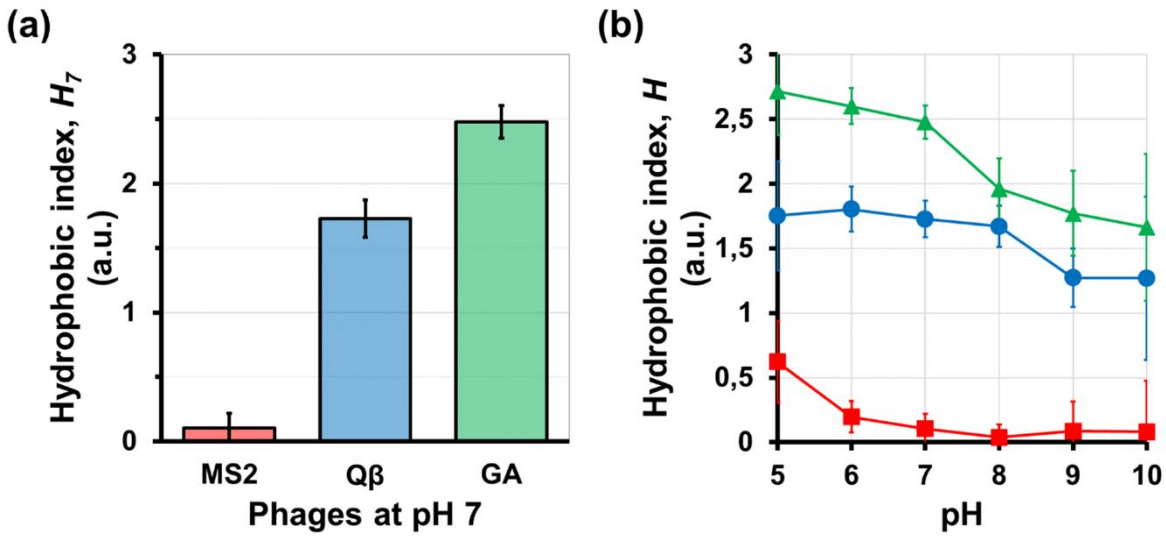

Fig. 4. Hydrophilic/hydrophobic balance for capsid protein of GA and MS2 phages. Hydrophobic amino acids provide positive score (+) while the hydrophilic ones provide negative score (-). Dotted line: MS2. Solid line: GA. Results obtained from the online 'protscale' software using a 'Kyte and Doolittle' algorithm and a smoothing average window through 7 amino acids. The primary sequences of capsid protein of GA and MS2 used are from the database 'UniprotKB' under reference #P07234 and #P03612 for GA and MS2, respectively.

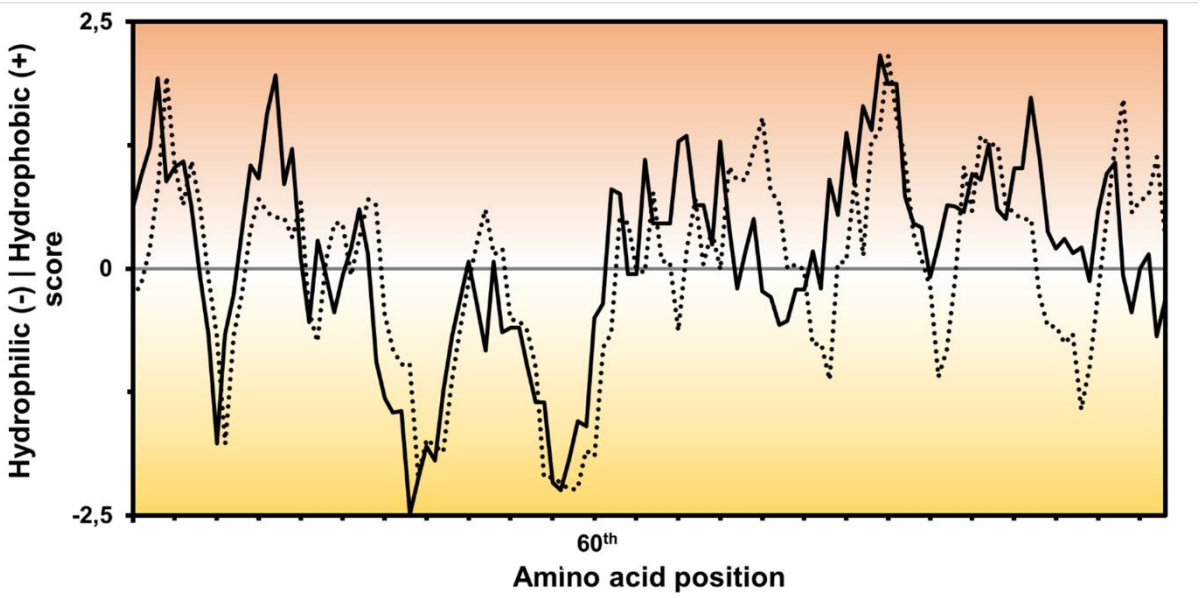

Fig. 5. Overlaps of phages hydrophobicity and native electrophoretic mobility as a function of pH. Hydrophobic indexes H_{pH}^{phage} (left axis, purple) and native electrophoretic mobilities $\mu_{native}^{phage,\ pH}$ (right axis, orange) of MS2 (left, ■), Qβ (middle, ●) and GA (right, ▲). Error bars are standard deviations (n=6 for hydrophobic index, n=3 for electrophoretic mobility).

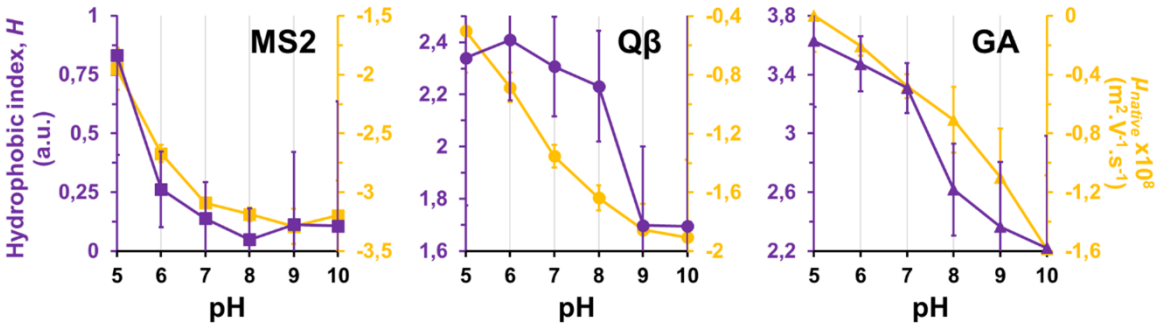

Supplementary Materials

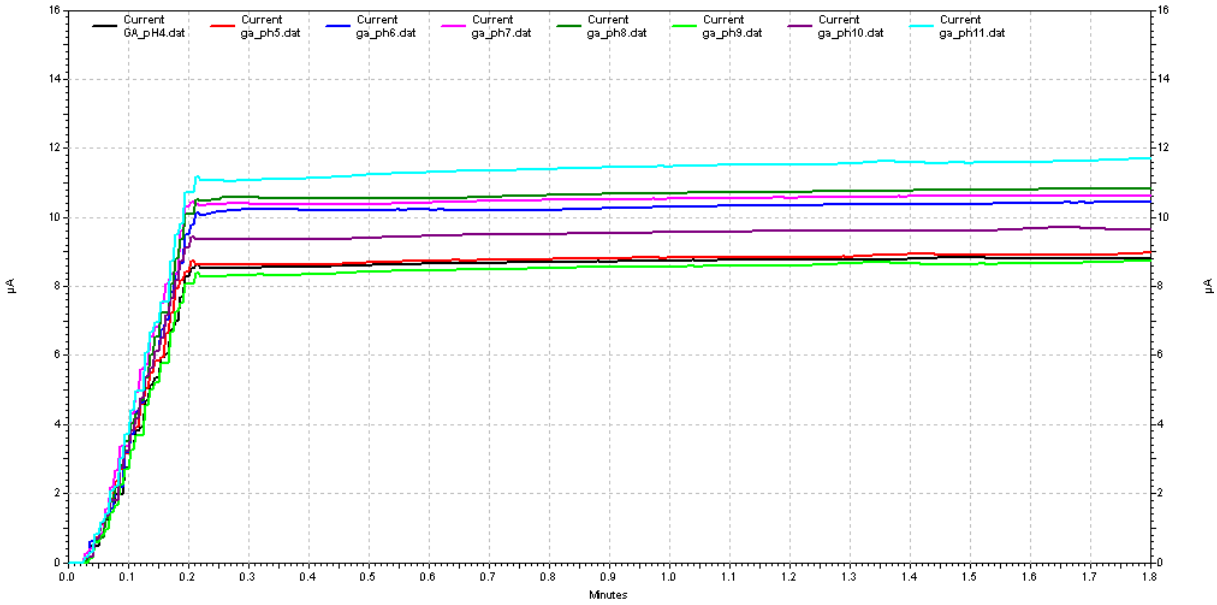

Figure S1. Current measured across the capillary for SDS-free BGEs. Results obtained by using BGEs at pH ranged from 4 to 11 (indicated on the graph). Please, read the Materials and Methods section for details about CE instrumental conditions (all runs having been performed similarly), and the Appendix A about the preparation of BGEs.

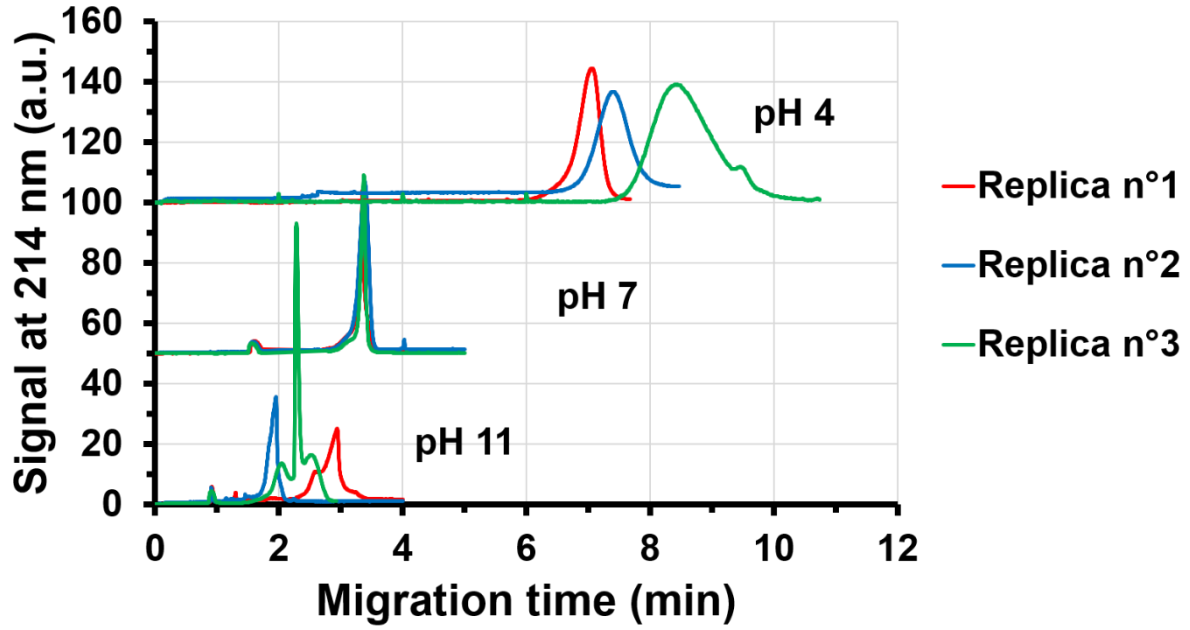

Figure S2. Repeated CE analyses of MS2 phage. Electropherograms recorded in triplicate (red, blue and green traces) by using 10 mM ionic strength BGEs adjusted at pH 4, 7 and 11 (indicated on the graph). Please, read the Materials and Methods section for details about CE instrumental conditions (all runs having been performed similarly), and the Appendix A about the preparation of BGEs.